

Bioprinting small-diameter vascular vessel with endothelium and smooth muscle by the approach of two-step crosslinking process

Qianheng Jin¹, Guangzhe Jin², Jihui Ju², Lei Xu², Linfeng Tang², Yi Fu³, Ruixing Hou², Anthony Atala⁴, and Weixin Zhao¹

¹Wake Forest Institute for Regenerative Medicine

²Ruihua affiliated hospital of Soochow University

³Soochow University Medical College

⁴Wake Forest School of Medicine

December 7, 2021

Abstract

Three-dimensional (3D) bioprinting shows great potential for autologous vascular grafts due to its simplicity, accuracy, and flexibility. 6mm diameter vascular grafts are used in clinic. However, producing small-diameter vascular grafts are still an enormous challenge. Normally, sacrificial hydrogels are used as temporary lumen support to mold tubular structure which will affect the structure's stability. In this study, we develop a new bioprinting approach to fabricating small-diameter vessel using two-step crosslinking process. $\frac{1}{4}$ lumen wall of bioprinted gelatin methacrylate (GelMA) flat structure is exposed to ultraviolet (UV) light briefly for having certain strength, while $\frac{3}{4}$ lumen wall shows as concave structure remained uncrosslinked. Pre-crosslinked flat structure is merged towards the uncrosslinked concave structure. Two individual structures will be combined tightly into an intact tubular structure by receiving more UV exposure time. Complicated tubular structures are constructed by these method. Notably, the GelMA-based bioink loaded with smooth muscle cells (SMCs) are bioprinted as the outer layer and human umbilical vein endothelial cells (HUVECs) are seeded onto the inner surface. A bionic vascular vessel with dual layers is fabricated successfully and keeps good viability, and functionality. This study may provide a novel idea for fabricating biomimetic vascular network or other more complicated organs.

Bioprinting small-diameter vascular vessel with endothelium and smooth muscle by the approach of two-step crosslinking process

Qianheng Jin^{1,2,#}, Jin Guangzhe^{2,#}, Jihui Ju², Lei Xu^{1,2}, Linfeng Tang², Yi Fu³, Ruixing Hou^{2,*}, Anthony Atala^{1,*}, Weixin Zhao^{1,*}

1 Wake Forest Institute for Regenerative Medicine, Wake Forest University School of Medicine, Winston-Salem, North Carolina 27157, USA

2 Department of Hand surgery, Ruihua affiliated hospital of Soochow University, Suzhou 215104, China

3 Department of Human Anatomy, Histology and Embryology, School of Biology and Basic Medical Sciences, Soochow University, Suzhou 215123, China

*Corresponding Author.

Weixin Zhao, MD. Wake Forest Institute for Regenerative Medicine, Wake Forest University School of Medicine, Winston Salem, NC 27157, USA.

mail: wezhao@wakehealth.edu

Anthony Atala, MD. Wake Forest Institute for Regenerative Medicine, Wake Forest University School of Medicine, Winston Salem, NC 27157, USA.

E-mail: aatala@wakehealth.edu

Ruixing Hou, Phd. Department of Hand surgery, Ruihua affiliated hospital of Soochow University, Suzhou 215104, China

mail: hrx2020@suda.edu.cn

These authors contributed equally to this work.

Funding information

National Natural Science Foundation of China, Grand/Award Number: 31900969;

Suzhou Municipal Science and Technology Bureau, Grand/Award Number: SYS202007;

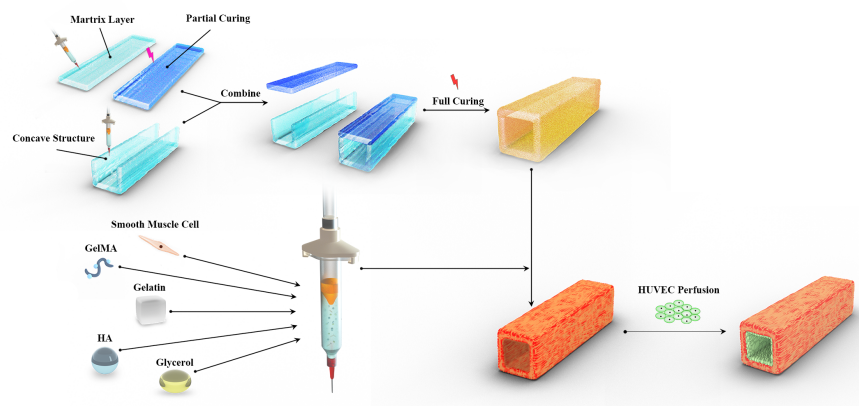
Suzhou Science and Education for Healthy, Grand/Award Number: KJXW2019073;

The Gusu Health Talent Training Project of Suzhou, Grand/Award Number: GSWS2019088.

Abstract

Three-dimensional (3D) bioprinting shows great potential for autologous vascular grafts due to its simplicity, accuracy, and flexibility. 6mm diameter vascular grafts are used in clinic. However, producing small-diameter vascular grafts are still an enormous challenge. Normally, sacrificial hydrogels are used as temporary lumen support to mold tubular structure which will affect the structure's stability. In this study, we develop a new bioprinting approach to fabricating small-diameter vessel using two-step crosslinking process. $\frac{1}{4}$ lumen wall of bioprinted gelatin methacrylate (GelMA) flat structure is exposed to ultraviolet (UV) light briefly for having certain strength, while $\frac{3}{4}$ lumen wall shows as concave structure remained uncrosslinked. Pre-crosslinked flat structure is merged towards the uncrosslinked concave structure. Two individual structures will be combined tightly into an intact tubular structure by receiving more UV exposure time. Complicated tubular structures are constructed by these method. Notably, the GelMA-based bioink loaded with smooth muscle cells (SMCs) are bioprinted as the outer layer and human umbilical vein endothelial cells (HUVECs) are seeded onto the inner surface. A bionic vascular vessel with dual layers is fabricated successfully and keeps good viability, and functionality. This study may provide a novel idea for fabricating biomimetic vascular network or other more complicated organs.

Graphical Abstract



Bioprinting small-diameter vascular vessel with endothelium and smooth muscle by the approach of two-step crosslinking process: Sacrificial hydrogels are used as temporary lumen support

to mold tubular structure which will affect the structure's stability. To avoid using the sacrificial hydrogel, we develop a new bioprinting approach to fabricating small-diameter vessel using two-step crosslinking process. Bioprinting the GelMA-based hydrogel containing Smooth muscle cell (SMCs) and perfused with human umbilical vein endothelial cells (HUVECs), a complicated bionic vascular vessel with dual layers is fabricated.

Key word: 3D bioprinting, Two-step crosslinking, Small-diameter vascular vessel, Tissue engineering, GelMA

1 Introduction

Cardiovascular diseases (CVDs) are considered the major cause of death world widely (Zoghbi et al., 2014). The main treatment methods include medical therapy, endovascular intervention, and surgical transplantation (Buchanan et al., 2014). Autologous blood vascular transplantation remains to be the gold standard for surgical transplantation (Rodriguez, Pavlovsky, & Del Pozo, 2016). Although surgical technique continues to be improved, the success rate of autologous blood vascular transplantation is only around 50% (de Vries, Simons, Jukema, Braun, & Quax, 2016). The reason for failure is the embolization of vessels due to the difference of diameter and mechanical properties between grafts and cardiovascular (Y. Zhang et al., 2017). Tissue engineered vascular grafts (TEVGs) have been explored as potential candidate for the treatment of CVDs. TEVGs, larger than 6mm has been widely used in cardiovascular surgery. However, due to the limitation of manufacturing technology, the construction of small-diameter blood vessel (SDBVs) grafts is still a challenge (Yamanaka, Yamaoka, Mahara, Morimoto, & Suzuki, 2018).

Most of the vessels are composed of three concentric layers: intima, media and adventitia (Elliott & Gerecht, 2016; Nemen-Guanzon et al., 2012). Intima is the innermost layer of vessels, which is consisted of a monolayer of endothelial cells. It directly contacts the blood and is a barrier between vessels and blood flow to prevent blood infiltration and thrombosis. The middle layer is composed of collagen I, collagen II, proteoglycan, elastin, and smooth muscle cells. Smooth muscle and collagen are arranged in a spiral pattern which is conducive to maintaining the elasticity and structural support. The adventitia is composed of fibroblasts and a loose collagen structure, which can keep the vascular structure intact and prevent tearing (Lesman, Rosenfeld, Landau, & Levenberg, 2016; Tomasina, Bodet, Mota, Moroni, & Camarero-Espinosa, 2019). There are many methods for making TEVGs, including electrospinning, phase separation, dissolution casting and so on (Jing et al., 2015; J. S. Miller et al., 2012; Pattanaik et al., 2019; Wang et al., 2018). These processes simulate blood vessels in mechanical properties, but they are still insufficient in biological properties.

3D bioprinting, a newly developed technology that integrates digital modeling, electromechanical control, information control, biomaterials, and chemistry, can accurately locate the cells and biomaterials into the complex multi-scale structure and simulate the complex tissue (Kolesky, Homan, Skylar-Scott, & Lewis, 2016; Murphy & Atala, 2014). In the past decade, 3D bioprinting has been widely used in the field of vascular regenerative medicine (Hong et al., 2020; Kolesky et al., 2014). Rotary bioprinting is a convenient method. Fibrin-based vascular structures are fabricated through a new self-designed rotary 3D bioprinter. During two months of the cultures, mechanical strength and collagen deposition are observed and the burst pressure of the structure reaches 52% of human saphenous vein (Freeman et al., 2019). Yet, the structure constructed in this way is relatively single, which cannot meet the complexity of natural vessels. 2 cm long, 4 mm diameter lumen heterogeneous bilayer bionic blood vessels are bioprinted by vertical stacking in one step. The dense inner layer containing HUVECs and the loose outer layer containing SMCs are formed by using the two separate concentrations of GelMA in different layers (Xu et al., 2020). The above research provides a theoretical possibility for us to create small-diameter vessels. However, there is also a big deficiency in this study. The construct is easy to collapse during the printing process due to the gravity of hydrogels, and the length and inner diameter of vessels are limited. Therefore, a new approach needs to be found to provide support and overcome these shortcomings.

Sacrificial hydrogels such as Agarose, gelatin and pluronic F127 are usually used to create complex tubular

structure. Pluronic F127 containing HUVECs and Ca²⁺ is used as the coaxial inner layer and catechol-functionalized, gelatin methacrylate (GelMA/C) containing SMCs is used as the coaxial outer layer. The GelMA/C undergoes rapid oxidative crosslinking in situ when touching the Ca²⁺ during the printing process and a vascular structure with high tissue affinity, perfusability and permeability is formed (Cui et al., 2019). Agarose is applied as the temporary support of the scaffold and various vascular cell types are successfully self-assembled by a rapid prototyping bioprinting method to form a vessel construct with controllable diameter (Norotte, Marga, Niklason, & Forgacs, 2009). Although sacrificial hydrogels can be used as a support in the bioprinting process, each sacrifice hydrogel has its own disadvantages. Agarose has a melting point of 60-70°C which will lead the cell destruction in the process of removal (Jordan S. Miller et al., 2012). Gelatin has poor mechanical property and cannot fulfill the support of complex structure. Due to good quality in printing and wonderful support property, pluronic F127 is used in common. However, the concentration of pluronic F127 used in the bioprinting needs to reach 30-40% which will lead the water separate out from the low concentration bioink. Thus, the accuracy of the structures and the cell viabilities will be affected (Wu, DeConinck, & Lewis, 2011).

Based on this, to overcome the defects of sacrificial hydrogel and improve the accuracy of the processing. We herein present a new approach to fabricating bilayer small-diameter vascular vessel without sacrifice bioink by using two-step crosslinking process. To achieve this, $\frac{1}{4}$ lumen wall of bioprinted GelMA-based flat structure were bioprinted and undergo a short time UV light curing to obtain a certain strength. Then the flat structure can be turned over to the uncrosslinked GelMA of concave structure. Treated with long time UV curing, the two independent structures can be combined. Through the experiments, we studied the properties of GelMA bioink with different crosslinking time first and investigate the connectivity of the two-step crosslinking structure. Furthermore, we fabricated complex small-diameter vascular vessels with HUVECs and SMCs by the two-step crosslinking method. To our knowledge, this work represents a new methodology for constructing complicated bionic vascular vessel.

2 Materials and Methods

2.1 Synthesis and identification of GelMA

The GelMA was synthesized in the following procedure (Xu et al., 2020). 8 g gelatin (type A, 300 bloom from porcine skin, Sigma-Aldrich, USA) was dissolved in 50 ml 0.25 M carbonate-bicarbonate buffer with pH 9.2 for 1 h. 0.8 ml of methacrylic anhydride (MA) (Sigma-Aldrich, USA) was slowly added into this solution, and allowed to react for 3 h at 700 RPM at 55. The reaction was terminated by the addition of 80 ml Dulbecco's phosphate buffered saline (DPBS), and the resulting solution was dialyzed in deionized water with 12-14 kDa cut-off dialysis tubes at 37 for 7 days. The deionized water was changed every morning and night. The solution was filtered and cooled at -20 for 1 hour, -80 for 2 hours, lyophilized for 5 days and stored at -20 freezer until use.

2.2 ¹H-Nuclear Magnetic Resonance (¹H-NMR) analysis

GelMA was confirmed by ¹H-NMR. 30 mg/ml GelMA was dissolved in deuterium oxide (D₂O) (Sigma-Aldrich, USA) at 40. ¹H-NMR spectra were obtained by NMR spectroscopy with a single axis gradient at 400 MHz (¹H-NMR, Bruker, Billerica, MA). Gelatin was used as a control.

2.3 Determination of TNBS

The methacrylation degree of GelMA was measured by 2,4,6-trinitrobenzenesulfonic acid (TNBS) (Sigma-Aldrich, USA) assay. GelMA was dissolved in sodium bicarbonate solution (pH = 8.5, 0.1 M) to obtain a concentration of 200 µg/ml. 250 µL of 0.01% w/v TNBS reaction solution was added to the sample solution and reacted at 37 for 2 hours. The reaction was terminated with 250 µL 10% sodium dodecyl sulfate (SDS) and 125 µL 1 N hydrochloric acid (HCl). 100 µL mixture was added into 96 well plate and optical density (OD) was obtained by microplate reader (SpectraMax M5, Molecular, USA) at 335nm. Gelatin was used as a control.

Degree of the methacrylation = (1-OD of GelMA / OD of Gelatin) × 100 (%)

2.4 FTIR analysis

GelMA was dissolved in DPBS at a concentration of 50 mg/ml for 2 hours at 37 °C. After GelMA was completely dissolved, 1 m/v 2-Hydroxy-4'-(2-hydroxyethoxy)-2-methylpropiophenone (Irgacure 2959, Sigma-Aldrich, USA) was added. The mixture was crosslinked for 5, 10, 20, 40, 60, 80 and 100s with the wavelength of 365 nm and the intensity of 200 mW/cm² to get different samples with different crosslinking time. The samples were lyophilized and analyzed by FTIR-ATR spectroscopy (Frontier, PerkinElmer, Rodgau, UK). All samples were scanned 5 times at 400-4000 cm⁻¹ with a resolution of 4 cm⁻¹. Gelatin was used as a control.

2.5 Preparation sample of GelMA solutions

GelMA solutions consisted of 50 mg/ml GelMA, 30 mg/ml Gelatin, 3.5 mg/ml sodium hyaluronate (HA), 10% v/v glycerol, and 1% m/v Irgacure 2959 in DPBS water. Gelatin and glycerol could increase the printability and HA could increase the biocompatibility of GelMA hydrogel (Xu et al., 2020). The mixture was cast in a mold and crosslinked for 5, 10, 20, 40, 60, 80, 100s under the UV light with a wavelength of 365 nm and the intensity of 200 mW/cm² to make a sample with 1 cm in diameter and 2 mm in thickness.

2.6 Rheological measurements

The mechanical properties of GelMA with different crosslinking times were analyzed by using a discovery hybrid rheometer dhr-2 (TA instruments, Newcastle, DE, USA). Frequency scanning was performed from 1 to 100 Hz with 1% constant strain. Strain scanning was performed from 0.01 to 3% rad/s at an oscillation frequency of 1Hz.

2.7 Swelling ratio and residual mass test

GelMA samples with different crosslinking times were weighed as (W₀) and gently shaken in DPBS and DI water at 37 °C for two days to remove the uncrosslinked GelMA. The swelling mass was recorded as (W_s) and the expanded samples were lyophilized to obtain the mass (W_r).

$$\text{Swelling ratio} = (W_s - W_r) / W_r \times 100\%$$

$$\text{Residual ratio} = W_r / (W_0 \times 5\%) \times 100\%$$

2.8 Scanning electron microscopy

The samples were placed in DI water at 37 °C for two days, cooled at -80 °C for 2 hours, and then lyophilized. The cross section of the structure was sputter coated with gold at 15 mA for 2 min (EM Ace600, Leica, Germany) and observed under a scanning electron microscope (SEM, Flex SEM1000, Hitachi, Japan) at 10kV. The diameters of different samples were analyzed using image J.

2.9 Combination of two step crosslinking

GelMA solution was added to one side of the mold (Fig. 3A). After crosslinked for 10 s, the solution was added to the other side and crosslinked for 100s to form a two-step crosslinked sample. GelMA solution was added to both sides of the mold and directly crosslinked for 100s was used as one-step crosslinked sample as a control.

Two-step crosslinked and one-step crosslinked samples were loaded in Instron mechanical tester (Model 5533, Instron Corporation, Norwood, Ma, USA), and tensile tests were conducted with a maximum value of 10N load cell.

Two-step crosslinked samples were observed by scanning electron microscope (SEM) to analyze the pore size and the integrity of connections.

2.10 Cell culture

Human umbilical vein endothelial cells (HUVECs, Lonza, MD, USA) were cultured in EGM-2 (Lonza, USA) and smooth muscle cells (SMCs, Lonza, MD, USA) were cultured in smooth muscle cell growth medium 2 (Promocell, USA). Both media were added with 1% v/v penicillin and streptomycin antibiotic and the

cells were cultured at 37 °C, 5% CO₂, and 95% relative humidity. 1:1 EGM-2 and smooth muscle cell growth medium were mixed for culturing the printed vascular structure, and the mixed medium was changed every two days. HUVECs and SMCs used in all experiments were in 4 to 8 generations.

2.11 3D bioprinting of vascular structure

3D bioprinting was conducted on a custom-made integrated tissue and organ printing (ITOP). In brief, the printer had a X, Y, and Z stage controllers, a distributing pneumatic pressure control system for accurately dispensing several materials within a single print. The bioprinter sat in a closed chamber which control temperature and humidity. It could deposit cell-laden hydrogels together with synthetic polymers and overcome the limitations on the size, shape, and structural integrity of single hydrogel prints and create customizable tissue.

For printing our constructs, we added 5% GelMA solution into the syringe with the nozzle of 300 μm (Izumi, Japan). The flat structure and the concave structure were printed with the pressure of 100 kPa and the feedrate of 60 mm/min. We crosslinked the flat structure under UV light for 10s to increase mechanical strength, then placed it on top of concave structure, and crosslinked this integrated structure for 100s to make the two individual structures combine unitedly (Fig 3E).

For the bionic vascular structure with cells, 10×10⁶SMCs were mixed into 5% GelMA solution, and then printed as described above. Prior to the seeding process, 50 μg/ml fibronectin (Invitrogen, USA) solution was injected into the channel to increase cell adhesion. HUVECs suspension (30×10⁶ cell/ml) was injected into the channel, and the structures were incubated at 37 °C for 2 hours. The structures were flipped every 30 minutes to permit cell attachment on all sides, which resulted in a monolayer of HUVECs on the channel wall(Freeman et al., 2019).

2.12 Cell viability and proliferation

The cell viability was assessed using a live/dead viability/cytotoxicity kit (Invitrogen, USA). Briefly, the vascular structure was washed 3 times with DPBS, and then incubated at 0.5 μL/ml Calcein AM and 2 μL/ml ethidium homodimer for 45 minutes. Laser confocal microscopy (LSI, Leica, Germany) was used to observe the living and dead cells in the structure. Six random views were selected to evaluate the cell viability using Image J.

CCK-8 (Sigma-Aldrich, USA) was used to detect the cell proliferation in the vascular structure. These vascular structures were transferred into a 24 well plate. 900 μL fresh medium and 100 μL CCK-8 solution were added. After incubated at 37 °C for 3 hours, 100 μL solution was transferred into 96 well plate and the ODs were read by spectramax M5 at 460nm.

2.13 Histological and immunofluorescence analysis

The vascular structures were fixed with 4% v/v paraformaldehyde after culture for 7 days and cut into 15μm section with a cryostat (CM1950, Leica, Germany) at -20 °C. Slices were stained with hematoxylin and eosin staining (H&E) and Masson's trichrome staining. Image were collected by light microscopy (DM4000b, Leica, Germany).

For immunofluorescence staining, HUVECs were labeled with mouse anti-human CD31 (1:50, Abcam, USA) and SMCs were labeled with rabbit anti-human α-SMA (1:200, Abcam, USA). Alexa Fluor 488 goat anti-mouse (1:500, Abcam, USA) and Alexa Fluor 594 Donkey anti-rabbit (1:500, Abcam, USA) were used as secondary antibodies. All the section were counterstained with DAPI. Fluorescence images were obtained with a fluorescent microscope (Leica, DM8000, Germany). The sections without primary antibody staining were used as control.

2.14 SEM of vascular structure

The 3D bionics vascular structure was fixed with 2.5% glutaraldehyde (Sigma-Aldrich, USA) at 4 °C for 4 hours after 7 days of culture. The structure was dehydrated with 30%, 50%, 70%, 80%, 90%, 95% and 100%

ethanol for 20 minutes each. After replacing the ethanol with CO₂ by a critical point dryer (Leica, EM CPD 300, Germany) and coating with gold, the samples were observed by SEM.

2.15 Statistical analysis

Data was processed by calculating means \pm SD (standard deviation). T-test was used to assess the differences between groups. $P < 0.05$ means significant difference (*, $P < 0.05$; **, $P < 0.01$; ***, $P < 0.001$; NS, not significant)

3 Results

3.1 Synthesis and identification of GelMA

The amino groups on gelatin were partly replaced by methacrylic acid to form GelMA with crosslinking ability (Bahcecioglu, Hasirci, Bilgen, & Hasirci, 2019). The synthetic GelMA was identified by ¹H-NMR (Figure S1). The characteristic resonance peak of the methacrylic acid group (5.5-6 ppm) appeared in GelMA, which is missing in the control. The substitution degree of GelMA was assessed to be $79.3 \pm 2.7\%$ by TNBS.

3.2 The effect of crosslinking time on GelMA properties

The number of double bonds in GelMA increased with increasing crosslinking time (Chen et al., 2012) (Figure 2A). Treated with different crosslinking time, GelMA showed different physical states. While the GelMA with only 5 s crosslinking time was changed from liquid to preliminary solid, which cannot maintain its shape for a longer time. However, samples with 10, 20 and 40 s crosslinking time maintained good shape (Figure 2B) lasting for long time.

Fourier transform infrared spectroscopy (FT-IR) was used to identify the correlation peaks in GelMA with different crosslinking times. A peak at 1525 cm^{-1} corresponded to C-N stretching and N-H bending; 1640 cm^{-1} to O-H bonding; 2922 cm^{-1} to C-H stretching; and 3300 cm^{-1} to O-H stretching. GelMA with different crosslinking times showed different peaks at these positions (Dursun Usal, Yucel, & Hasirci, 2019). We evaluated the FTIR of gelatin, uncrosslinked GelMA, and GelMA with different crosslinking times. The peaks of the two amino groups at 1540 and 1640 cm^{-1} in uncrosslinked GelMA were significantly increased compare with gelatin, which indicated that the amino groups in gelatin were successfully replaced by methacrylic acid. After UV irradiation for different times, the two peaks gradually decreased. In addition, the -OH stretching vibrations at 3300 cm^{-1} also decreased, which was related to the decrease of total -OH caused by UV curing (Figure 2C).

GelMA with different crosslinking time was shaken in DI water at 37 °C for two days. The uncrosslinked GelMA was removed, and the remaining GelMA in the structure expanded which led to the pore size increasing (Figure 2D). The average pore sizes were 292.2 ± 25.00 (5 s), 308.9 ± 23.53 (10 s), 175.8 ± 15.66 (20 s), 85.06 ± 8.977 (40 s), 82.07 ± 9.089 (100 s) (Figure 2E). Gelatin, glycerin, and hyaluronic acid contained in crosslinked GelMA bioink will not affect the pore sizes of the constructs.

In order to characterize the physical properties of GelMA bioink with different crosslinking times, oscillatory rheological measurements were used. The storage modulus (G') and viscosity coefficient of GelMA bioink increased with the crosslinking time, and these kept steady when the crosslinking time reached 40 s (Figure 2F-G). In a certain range, the storage modulus remained stable with changing of frequencies and strains, which indicated the structure of crosslinked GelMA was stable under the shear force (Figure 2H-I). In addition, the storage modulus of GelMA bioink at each crosslinking time was much greater than the loss modulus which indicated that crosslinked GelMA was in a solid state (Figure 2J).

GelMA bioink with different crosslinking times showed different swelling ratios in DPBS and DI water. GelMA's swelling ratio was 23 times in DPBS with 5 and 10 s crosslinking times. With increasing of crosslinking time, the swelling ratio decreased. The swelling ratio was 17.5 times with 20s crosslinking time, and it was 15 times with 40s at which point it stabilized (Figure 2K). The swelling ratio was more remarkable in DI water. The swelling ratio was 400 times in 5 and 10 s, 200 times with 20 s and closed to 100 times

with 40 s (Figure 2L). This trend indicated that an increased number of double bonds result in a more stable framework.

The residual mass indicated the amount of residual GelMA in structure. With the increased of crosslinking time, residual mass increased gradually. The average residual masses obtained were 75.32 \pm 2.12% (5 s), 86.16 \pm 0.95% (10 s), 94.34 \pm 1.16% (20 s), 97.79 \pm 0.44% (40 s), 97.65 \pm 1.221% (60 s), 80s is 98.05 \pm 0.05% (80 s), and 97.18 \pm 0.45% (100 s) (Figure 2M).

3.3 Combination of two-step crosslinking approach

Two-step crosslinking resulted in substantial cohesion. Figure 3A showed that 10 s pre-crosslinked GelMA can be re-crosslinked with uncrosslinked GelMA bioink and formed a united combination. There was no sign of splitting at the combining site under the SEM observation (Figure 3b). In tensile loading, there was no significant difference in Young's modulus and tensile strain between structures formed by one-step or two-step crosslinking methods ($P > 0.05$) (Figure 3C-3D).

3.4 Fabrication of complicated tubular structures

We used the two-step crosslinking approach to fabricating a tubular structure of GelMA. The method of two-step crosslinking to construct tubular structure was showed in Figure 3E. Figure 3F showed the tubular construct with different diameters (0.08-0.2mm in lumen diameter and 0.6 mm in wall thickness). A 6 mm long tubular construct was showed in Figure 3G. SEM showed that the tubular structure has good bonding properties (Figure 3H).

Complicated designs demonstrated the advantages of two-step crosslinking method. We printed multiple curved tubular structure, branched tubular structure, circular tubular structure with single inlet/outlet, and several letters (Figure 4). Red inks were injected into these structures to show the connected channels within each structure and to demonstrate their integrity of fluid flow.

3.5 Cellular vessel structures

SMCs were added into GelMA which was acting as bioink to form the wall of vessel structure; while HUVECs were perfused into the inner space of vessel lumen to form a biomimetic barrier between blood and vessel wall.

The viabilities of SMCs and HUVECs in the vascular structure were analyzed by live/dead staining. The fluorescence images of 1, 4 and 7 days were obtained by confocal microscope. The cells were in granular state at the first day after printing. On the fourth day, the number of cells began to increase, and some cells began to expand in their shape. Most cells expanded and SMCs showed the long spindle shape in 7 days (Figure 5A). The cell survival rates were 93.64 \pm 1.455 (day 1), 91.62 \pm 2.070 (day 4), and 95.62 \pm 1.312 (day 7). All the survival rates in the structures were more than 90% (Figure 5B). CCK-8 was used to analyze cell proliferation. The CCK-8 absorption values of HUVECs and SMCs on day 0, 1, 4 and 7 were 0.110 \pm 0.0138, 0.110 \pm 0.0068, 0.209 \pm 0.0121 and 0.315 \pm 0.0179, respectively (Figure 5C). Cells significantly proliferated in the vascular structures.

H&E and Masson's trichrome staining were used for morphological detection, and immunofluorescence was used for functional assessment. After one week of culture, spreading out SMCs were well distributed in the outer layer. HUVECs formed a monolayer cell coverage on the inner lumen surface (Figure 5D-5E). CD31 and α -SMA immunofluorescence confirmed an inner endothelial layer and the outer smooth muscle layer from the vascular structure.

The morphology of the outer, middle, and inner layers of GelMA vascular construct in were further observed by SEM. Interestingly, the SMCs in the outer layer and middle layer were spreading out and arranged linearly along the vertical direction of printing. The HUVECs in the inner layers attached tightly to the surface of GelMA lumen surface and expanded to form a smooth barrier evenly.

4 Discussion

Scientists have been rapidly developing tissue engineered artificial blood vessels in the past decade, and used multiple ways to construct them (Morin, Smith, Davis, & Tranquillo, 2013). 3D bioprinting has become a research hotspot because of precision spatial control and uniform cell distribution (Hong et al., 2020). 3D bioprinting is a rapid prototyping and additive manufacturing technology, which considers various design aspects such as imaging, modeling, printer selection, bioink selection, culture conditions and 3D structure (Murphy & Atala, 2014; Y. S. Zhang, Oklu, Dokmeci, & Khademhosseini, 2018). However, there are still difficulties in the fabrication of complicated small-diameter blood vessels. The accuracy of 3D printing technology is limited in some scenarios for medical application, and current bioinks have various limitations in the most targeted applications. Printable materials with good biocompatibility tended to have poor mechanical properties. In bioprinting matrix loss and structural collapse often lead to failure of the printed construct (Ozbolat & Hospodiuk, 2016).

Normally, sacrificial hydrogels offer a temporary support in the fabrication of small-diameter vessels. But all sacrificial hydrogels have disadvantages (Bertassoni et al., 2014; Tocchio et al., 2015). Therefore, we developed a two-step crosslinking method to fabricate tunable structures. This method avoids the use of sacrificial hydrogels and produces a vessel structure with using single photocurable hydrogel – GelMA.

Hydrogel, as a material for loading cells and supporting structures, is particularly important in 3D bioprinting (Hoelzl et al., 2016). An ideal hydrogel needs to have biological and mechanical properties similar to its intended tissue and should be adaptable to the printing process. In addition, hydrogel structures need to facilitate cell proliferation and differentiation after bioprinting. Naturally derived hydrogels (including agarose, alginate, collagen, fibrin, gelatin and hyaluronic acid) provide an effective growth environment for cells (Cui, Nowicki, Fisher, & Zhang, 2017). However, these hydrogels lack sufficient mechanical strength to create the complicated 3D structure of a tubular structure. GelMA as a biocompatible polymer is produced by modified gelatin with methacrylic anhydride (MA), and is able to be crosslinked with UV light to obtain higher physical strength (Liu & Chan-Park, 2010). Our preliminary experiments showed that uncrosslinked GelMA hydrogel can be stacked up to 20 printed layers. In this study, 5% m/v GelMA was used to fabricate the tubular structure. The pore size at this concentration could hold SMCs in the spot of three dimensional space, and was beneficial to the proliferation of the cells (Jeong et al., 2007). We compared the properties of GelMA solution with different curing time. Although GelMA with 5 s crosslinking could get semisolid immediately, it could not keep its shape for a longer time. 10 s crosslinking time for the GelMA was used at the first crosslinking step due to maintain its spatial form, open the least double bonds, and then lay a proper foundation for the second crosslinking step. Moreover, the water absorption capacity of GelMA with 5 s and 10 s crosslinking time could reach 400 times of its own mass in DI water, and its volume also expands accordingly. Therefore, the low degree of crosslinked GelMA was also a good swelling material to be applied in the investigation of tissue engineering.

Pre-crosslinking can enhance the physical property of photocurable hydrogel. In the process of vertical bioprinting, the printed bottom GelMA bioink was partly crosslinked by continuous UV light to avoid cell leakage and structure collapse (Xu et al., 2020). A user-defined, complexity cell-laden channel was fabricated by a sequential printing approach. The photocurable hydrogels were briefly exposed layer-by-layer to increase support performance. The sacrificial hydrogels were printed into the desired layer and fully crosslinked. With the removal of sacrificial hydrogels, precise and complex channels could be constructed (Ji, Almeida, & Guvendiren, 2019). In our study, GelMA was made semisolid after first-step crosslinking process. The semisolid GelMA with required physical strength could be bonded tightly with uncrosslinked GelMA. The combination was received second-step crosslinking process which produced a longer UV exposure time. A bionic vascular vessel with small diameter was built successfully with using the two-step crosslinking method, which maintains consecutive tubular structure.

Furthermore, this method might be not only suitable for vessels, but also for other complicated structures such as hepatic sinusoid, nephron and pulmonary alveoli. The hydrogel can be partly cured, and the two-step curing can integrate two independent parts into a whole. This method may be suitable to photocurable hydrogel with better mechanical properties and make structures that are difficult to be formed in one step by

forming them in two or more steps. In addition, different kinds of photocuring materials containing double bonds may also be used with this two-step crosslinking method. In this way, we could make the connection between different tissues in bioprinting, such as the superior vena cava bioprinted by one photocuring material connected with the heart which is bioprinted by another photocuring material.

Human blood vascular vessel have three distinct layers: intima (endothelial cells), media (smooth muscle cells), and externa (fibroblasts) (Tomasina et al., 2019). We created a small diameter vascular structure ($\varnothing < 6\text{mm}$) with the spatial distribution of two different cells, which include bioprinted SMCs within bioink and subsequent perfusion of HUVECs into the lumen space. SMCs could aggregate, spread out, and proliferate to form outer layer of the construct, in that rich collagen area was found. Perfused HUVECs formed the connected inner layer that covers entire intraluminal surface with dense junctions. The SMCs were lined longitudinally along the structure which may be caused by axial traction during printing. During the culture of bioprinted vessel structure, the previous inner square shape turned to smooth gradually, that has been reported in previously publication (Esch, Post, Shuler, & Stokol, 2011).

Through this two-step crosslinking method, we have successfully bioprinted multiple complicated tubular structures and bionics vessels with inner monolayer endothelium surrounded by outer layer SMCs. This is a new fabrication method for tissue engineering of small diameter vessel. In addition, the alternatives of two-step crosslinking method might be adopted to create more complex structures.

5 Conclusion

We proposed a new approach to making small diameter vessels with complicated patterns and special cell distribution. The two-step crosslinking method created a continuous connection between different printed parts and resulted an intact tubular structure with biological advantages, as well proper sealing and mechanical properties. We accomplished this method by the investigation of GelMA properties varied by crosslinking time and optimized by crosslinking process. We fabricated a small vessel that possesses printed outer layer of SMCs and perfused inner layer of HUVECs by GelMA bioink printing and two-step crosslinking process. We also observed that the SMCs and HUVECs were expanded, proliferated, and functionalized during post printing culture. Our study might provide a new fabrication method for the construction of small diameter vessel with clinically relevant size and characteristics.

Conflict of Interest

All authors declare no conflict of interest.

Acknowledgements

This work was mainly supported by a grant from the state of North Carolina (NC), USA, the National Natural Science Foundation of China (31900969), Suzhou Municipal Science and Technology Bureau (SYS2020071), Suzhou Science and Education for Healthy (KJXW2019073) and the Gusu Health Talent Training Project of Suzhou (GSWS2019088).

Author Contributions

Weixin Zhao and Anthony Atala conceived and supervised the study. Weixin Zhao

and Ruixin Hou designed experiments. Qianheng Jin performed experiments. Qianheng Jin and Guangzhe Jin wrote the manuscript. Weixin Zhao revised the manuscript. Guangzhe Jin, Jihui Ju, Lei Xu, Linfeng Tang, Yi Fu analyzed data, and commented on the manuscript.

Data Availability Statement

The data that support the findings of this study are available from the corresponding author upon reasonable request.

Reference

- Bahcecioglu, G., Hasirci, N., Bilgen, B., & Hasirci, V. (2019). A 3D printed PCL/hydrogel construct with zone-specific biochemical composition mimicking that of the meniscus. *Biofabrication*, *11* (2). doi:10.1088/1758-5090/aaf707
- Bertassoni, L. E., Cecconi, M., Manoharan, V., Nikkhah, M., Hjortnaes, J., Cristino, A. L., . . . Khademhosseini, A. (2014). Hydrogel bioprinted microchannel networks for vascularization of tissue engineering constructs. *Lab Chip*, *14* (13), 2202-2211. doi:10.1039/c4lc00030g
- Buchanan, G. L., Chieffo, A., Meliga, E., Mehran, R., Park, S. J., Onuma, Y., . . . Colombo, A. (2014). Comparison of percutaneous coronary intervention (with drug-eluting stents) versus coronary artery bypass grafting in women with severe narrowing of the left main coronary artery (from the Women-Drug-Eluting stent for Left main coronary Artery disease Registry). *Am J Cardiol*, *113* (8), 1348-1355. doi:10.1016/j.amjcard.2014.01.409
- Chen, Y. C., Lin, R. Z., Qi, H., Yang, Y., Bae, H., Melero-Martin, J. M., & Khademhosseini, A. (2012). Functional Human Vascular Network Generated in Photocrosslinkable Gelatin Methacrylate Hydrogels. *Adv Funct Mater*, *22* (10), 2027-2039. doi:10.1002/adfm.201101662
- Cui, H., Nowicki, M., Fisher, J. P., & Zhang, L. G. (2017). 3D Bioprinting for Organ Regeneration. *Adv Healthc Mater*, *6* (1). doi:10.1002/adhm.201601118
- Cui, H., Zhu, W., Huang, Y., Liu, C., Yu, Z. X., Nowicki, M., . . . Zhang, L. G. (2019). In vitro and in vivo evaluation of 3D bioprinted small-diameter vasculature with smooth muscle and endothelium. *Biofabrication*, *12* (1), 015004. doi:10.1088/1758-5090/ab402c
- de Vries, M. R., Simons, K. H., Jukema, J. W., Braun, J., & Quax, P. H. (2016). Vein graft failure: from pathophysiology to clinical outcomes. *Nat Rev Cardiol*, *13* (8), 451-470. doi:10.1038/nrcardio.2016.76
- Dursun Usal, T., Yucel, D., & Hasirci, V. (2019). A novel GelMA-pHEMA hydrogel nerve guide for the treatment of peripheral nerve damages. *International journal of biological macromolecules*, *121* , 699-706. doi:10.1016/j.ijbiomac.2018.10.060
- Elliott, M. B., & Gerecht, S. (2016). Three-dimensional culture of small-diameter vascular grafts. *J Mater Chem B*, *4* (20), 3443-3453. doi:10.1039/c6tb00024j
- Esch, M. B., Post, D. J., Shuler, M. L., & Stokol, T. (2011). Characterization of In Vitro Endothelial Linings Grown Within Microfluidic Channels. *Tissue Engineering Part A*, *17* (23-24), 2965-2971. doi:10.1089/ten.tea.2010.0371
- Freeman, S., Ramos, R., Alexis Chando, P., Zhou, L., Reeser, K., Jin, S., . . . Ye, K. (2019). A bioink blend for rotary 3D bioprinting tissue engineered small-diameter vascular constructs. *Acta Biomater*, *95* , 152-164. doi:10.1016/j.actbio.2019.06.052
- Hoelzl, K., Lin, S., Tytgat, L., Van Vlierberghe, S., Gu, L., & Ovsianikov, A. (2016). Bioink properties before, during and after 3D bioprinting. *Biofabrication*, *8* (3). doi:10.1088/1758-5090/8/3/032002
- Hong, H., Seo, Y. B., Kim, D. Y., Lee, J. S., Lee, Y. J., Lee, H., . . . Park, C. H. (2020). Digital light processing 3D printed silk fibroin hydrogel for cartilage tissue engineering. *Biomaterials*, *232* , 119679. doi:10.1016/j.biomaterials.2019.119679
- Jeong, S. I., Kim, S. Y., Cho, S. K., Chong, M. S., Kim, K. S., Kim, H., . . . Lee, Y. M. (2007). Tissue-engineered vascular grafts composed of marine collagen and PLGA fibers using pulsatile perfusion bioreactors. *Biomaterials*, *28* (6), 1115-1122. doi:10.1016/j.biomaterials.2006.10.025
- Ji, S., Almeida, E., & Guvendiren, M. (2019). 3D bioprinting of complex channels within cell-laden hydrogels. *Acta Biomaterialia*, *95* , 214-224. doi:10.1016/j.actbio.2019.02.038
- Jing, X., Mi, H. Y., Salick, M. R., Cordie, T. M., Peng, X. F., & Turng, L. S. (2015). Electrospinning thermoplastic polyurethane/graphene oxide scaffolds for small diameter vascular graft applications. *Mater*

Sci Eng C Mater Biol Appl, 49 , 40-50. doi:10.1016/j.msec.2014.12.060

Kolesky, D. B., Homan, K. A., Skylar-Scott, M. A., & Lewis, J. A. (2016). Three-dimensional bioprinting of thick vascularized tissues. *Proc Natl Acad Sci U S A*, 113 (12), 3179-3184. doi:10.1073/pnas.1521342113

Kolesky, D. B., Truby, R. L., Gladman, A. S., Busbee, T. A., Homan, K. A., & Lewis, J. A. (2014). 3D bioprinting of vascularized, heterogeneous cell-laden tissue constructs. *Adv Mater*, 26 (19), 3124-3130. doi:10.1002/adma.201305506

Lesman, A., Rosenfeld, D., Landau, S., & Levenberg, S. (2016). Mechanical regulation of vascular network formation in engineered matrices. *Adv Drug Deliv Rev*, 96 , 176-182. doi:10.1016/j.addr.2015.07.005

Liu, Y., & Chan-Park, M. B. (2010). A biomimetic hydrogel based on methacrylated dextran-graft-lysine and gelatin for 3D smooth muscle cell culture. *Biomaterials*, 31 (6), 1158-1170. doi:10.1016/j.biomaterials.2009.10.040

Miller, J. S., Stevens, K. R., Yang, M. T., Baker, B. M., Nguyen, D.-H. T., Cohen, D. M., . . . Chen, C. S. (2012). Rapid casting of patterned vascular networks for perfusable engineered three-dimensional tissues. *Nature Materials*, 11 (9), 768-774. doi:10.1038/nmat3357

Miller, J. S., Stevens, K. R., Yang, M. T., Baker, B. M., Nguyen, D. H., Cohen, D. M., . . . Chen, C. S. (2012). Rapid casting of patterned vascular networks for perfusable engineered three-dimensional tissues. *Nat Mater*, 11 (9), 768-774. doi:10.1038/nmat3357

Morin, K. T., Smith, A. O., Davis, G. E., & Tranquillo, R. T. (2013). Aligned human microvessels formed in 3D fibrin gel by constraint of gel contraction. *Microvasc Res*, 90 , 12-22. doi:10.1016/j.mvr.2013.07.010

Murphy, S. V., & Atala, A. (2014). 3D bioprinting of tissues and organs. *Nat Biotechnol*, 32 (8), 773-785. doi:10.1038/nbt.2958

Nemeno-Guanzon, J. G., Lee, S., Berg, J. R., Jo, Y. H., Yeo, J. E., Nam, B. M., . . . Lee, J. I. (2012). Trends in tissue engineering for blood vessels. *J Biomed Biotechnol*, 2012 , 956345. doi:10.1155/2012/956345

Norotte, C., Marga, F. S., Niklason, L. E., & Forgacs, G. (2009). Scaffold-free vascular tissue engineering using bioprinting. *Biomaterials*, 30 (30), 5910-5917. doi:10.1016/j.biomaterials.2009.06.034

Ozbolat, I. T., & Hospodiuk, M. (2016). Current advances and future perspectives in extrusion-based bioprinting. *Biomaterials*, 76 , 321-343. doi:10.1016/j.biomaterials.2015.10.076

Pattanaik, S., Arbra, C., Bainbridge, H., Dennis, S. G., Fann, S. A., & Yost, M. J. (2019). Vascular Tissue Engineering Using Scaffold-Free Prevascular Endothelial-Fibroblast Constructs. *BioResearch open access*, 8 (1), 1-15. doi:10.1089/biores.2018.0039

Rodriguez, A. E., Pavlovsky, H., & Del Pozo, J. F. (2016). Understanding the Outcome of Randomized Trials with Drug-Eluting Stents and Coronary Artery Bypass Graft in Patients with Multivessel Disease: A Review of a 25-Year Journey. *Clin Med Insights Cardiol*, 10 , 195-199. doi:10.4137/CMC.S40645

Tocchio, A., Tamplenizza, M., Martello, F., Gerges, I., Rossi, E., Argenti, S., . . . Lenardi, C. (2015). Versatile fabrication of vascularizable scaffolds for large tissue engineering in bioreactor. *Biomaterials*, 45 , 124-131. doi:10.1016/j.biomaterials.2014.12.031

Tomasina, C., Bodet, T., Mota, C., Moroni, L., & Camarero-Espinosa, S. (2019). Bioprinting Vasculature: Materials, Cells and Emergent Techniques. *Materials (Basel)*, 12 (17). doi:10.3390/ma12172701

Wang, W., Nie, W., Zhou, X., Feng, W., Chen, L., Zhang, Q., . . . He, C. (2018). Fabrication of heterogeneous porous bilayered nanofibrous vascular grafts by two-step phase separation technique. *Acta Biomater*, 79 , 168-181. doi:10.1016/j.actbio.2018.08.014

Wu, W., DeConinck, A., & Lewis, J. A. (2011). Omnidirectional Printing of 3D Microvascular Networks. *Advanced Materials*, 23 (24), H178-H183. doi:10.1002/adma.201004625

Xu, L., Varkey, M., Jorgensen, A., Ju, J., Jin, Q., Park, J. H., . . . Atala, A. (2020). Bioprinting small diameter blood vessel constructs with an endothelial and smooth muscle cell bilayer in a single step. *Biofabrication*, *12* (4), 045012. doi:10.1088/1758-5090/aba2b6

Yamanaka, H., Yamaoka, T., Mahara, A., Morimoto, N., & Suzuki, S. (2018). Tissue-engineered submillimeter-diameter vascular grafts for free flap survival in rat model. *Biomaterials*, *179* , 156-163. doi:10.1016/j.biomaterials.2018.06.022

Zhang, Y., Li, X. S., Guex, A. G., Liu, S. S., Muller, E., Malini, R. I., . . . Spano, F. (2017). A compliant and biomimetic three-layered vascular graft for small blood vessels. *Biofabrication*, *9* (2), 025010. doi:10.1088/1758-5090/aa6bae

Zhang, Y. S., Oklu, R., Dokmeci, M. R., & Khademhosseini, A. (2018). Three-Dimensional Bioprinting Strategies for Tissue Engineering. *Cold Spring Harbor Perspectives in Medicine*, *8* (2). doi:10.1101/cshperspect.a025718

Zoghbi, W. A., Duncan, T., Antman, E., Barbosa, M., Champagne, B., Chen, D., . . . Wood, D. A. (2014). Sustainable development goals and the future of cardiovascular health: a statement from the Global Cardiovascular Disease Taskforce. *Glob Heart*, *9* (3), 273-274. doi:10.1016/j.gheart.2014.09.003

Figure 1

Schematic showing the novel printing method to create a small diameter tubular construct and the process of bioprinting a bionic vascular.

Figure 2

The analysis of GelMA hydrogel with different crosslinking times. (A) Schematics of GelMA polymer structure connections with different crosslinking times. (B) Gross images of GelMA with different crosslinking time. (C) FTIR of GelMA, Long time crosslinking GelMA, Short time crosslinking GelMA. (D) The SEM of the GelMA samples at 5s, 10s, 20s, 40s, 60s crosslinking time. (E) Pore size assessment of the GelMA samples at 5s, 10s, 20s, 40s, 60s crosslinking time. (***, $P < 0.001$; NS, not significant) Scale bar: 150 μm . (F, G) Storage modulus and Complex viscosity of the GelMA samples at different crosslinking times. (H, I) The storage modulus of the GelMA samples at different crosslinking times varying with Angular frequency and Strain. (J) The comparison of storage modulus and loss modulus of the GelMA samples at 5s, 10s, 20s, 40s crosslinking time. (K, L) The swelling ratio of the GelMA samples at different crosslinking times in DPBS and DI water. (M) The residual mass of the GelMA samples at different crosslinking times. (n=6)

Figure 3

The combining site of the samples with two-step crosslinking method and the appearance of tubular structure. (A) Gross image of the construct made by two-step crosslinking. Scale bar: 2mm. (B) The SEM of the construct made by two-step crosslinking (The red arrow refers to the combining site). Scale bar: 200 μm . (C) The stress-strain curves of one-step crosslinking structure and two-step crosslinking structure. (n=6) (D, E) The tensile strain and Young's Modulus of one-step crosslinking structure and two-step crosslinking structure. (n=6, NS, not significant). (E) The process of constructing a tubular structure. Scale bar: 2mm. (F) The tubular structures with different diameter. (G) 6 cm length tubular structure. (H) SEM of tubular structure. (The red arrow refers to the combining site). Scale bar: 200 μm .

Figure 4

3D complex tubular structure made by two-step crosslinking method. (A, B, C) Multiple curved, branched, and circular tubular structure with single inlet/outlet. (D) Printed letter with tubular structure. All structures were injected with a red ink for the approval of good sealing and patency. Scale bar: 2mm.

Figure 5

Cell viability, proliferation, and histology of bionic vascular vessel. (A) Live/dead staining of bionic vascular vessel (Day 1, Day 4 and Day 7). Scale bar: 200 μm . (B) Cell viability of bionic vascular. (C) Cell proliferation by CCK-8 assay ($n=4$, **, $P < 0.01$; 0.01***, $P < 0.001$; NS, not significant). (D, E) The H&E staining and Masson staining.

Figure 6

Immunofluorescence and SEM of bionic vascular vessel. (A) Immunofluorescence of bionic vascular vessel. (CD31, green; α -sma, red; DAPI, blue). (B) SEM of bionic vascular vessel. HUVECs attached on the intraluminal surface, and SMCs were distributed linearly within the wall of the structure.

Figure support 1

The $^1\text{H-NMR}$ of GelMA and Gelatin. The characteristic resonance peak of the methacrylic acid group (5.5-6 ppm) appeared in GelMA, which is missing in the Gelatin.

Figure 1

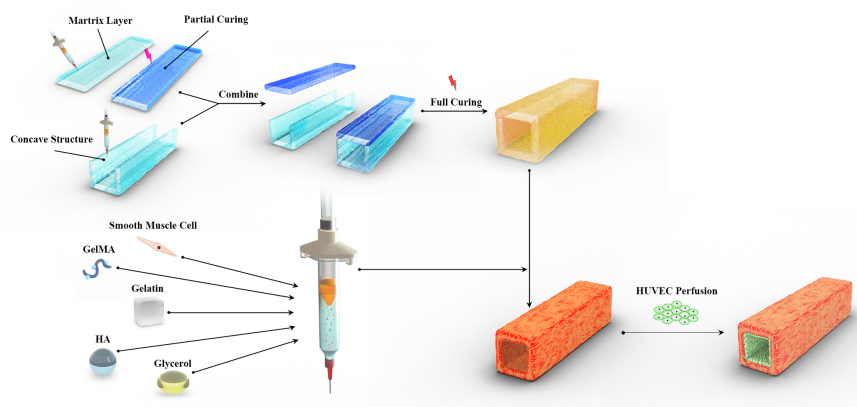


Figure 2

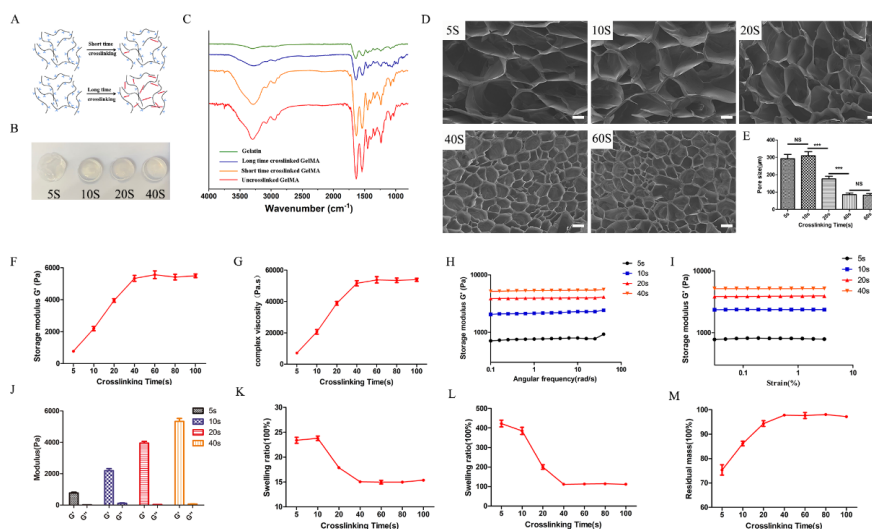


Figure 3

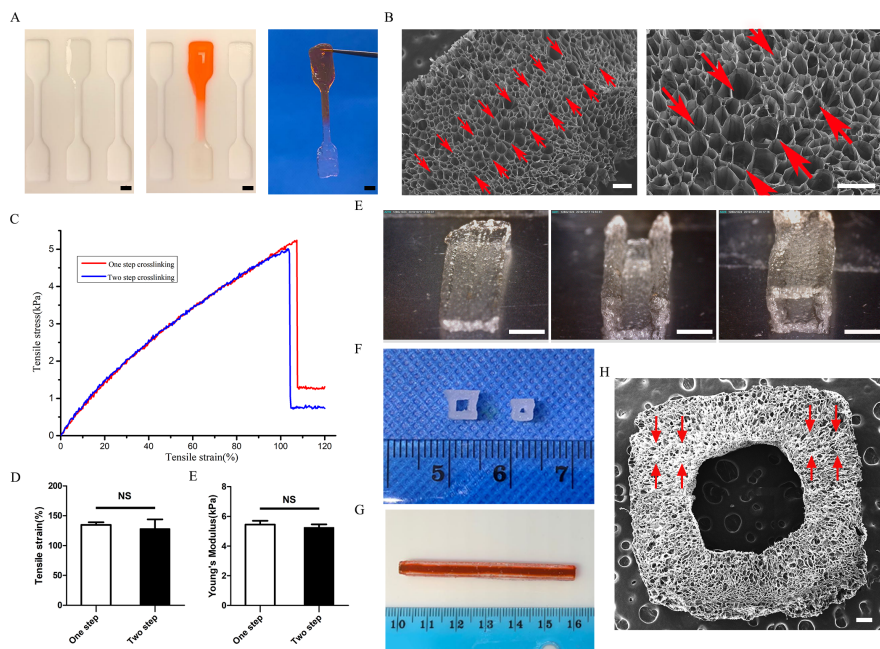


Figure 4

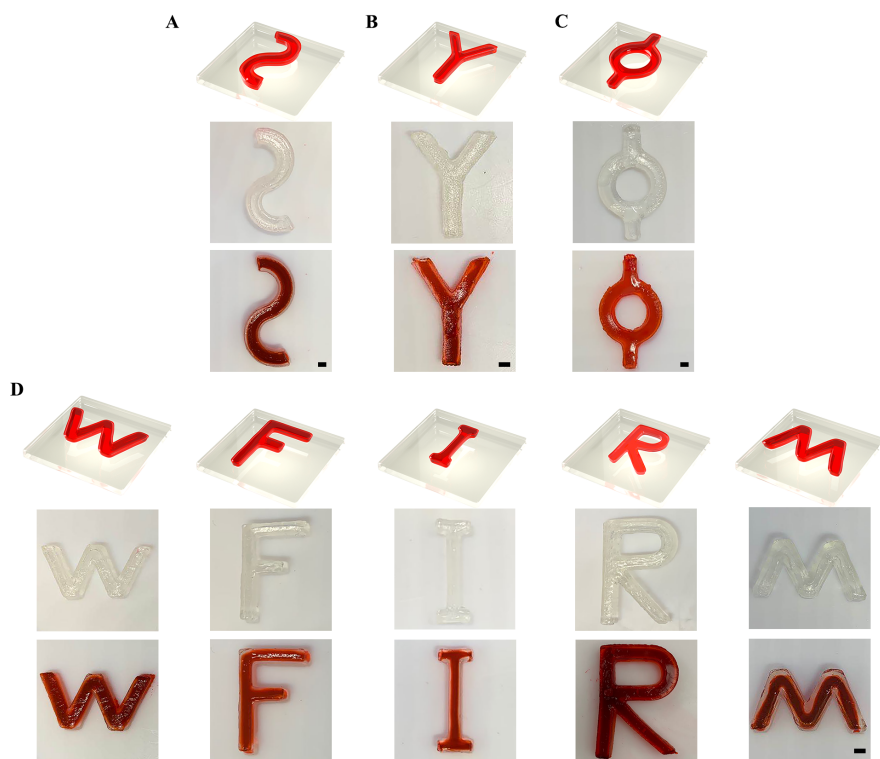


Figure 5

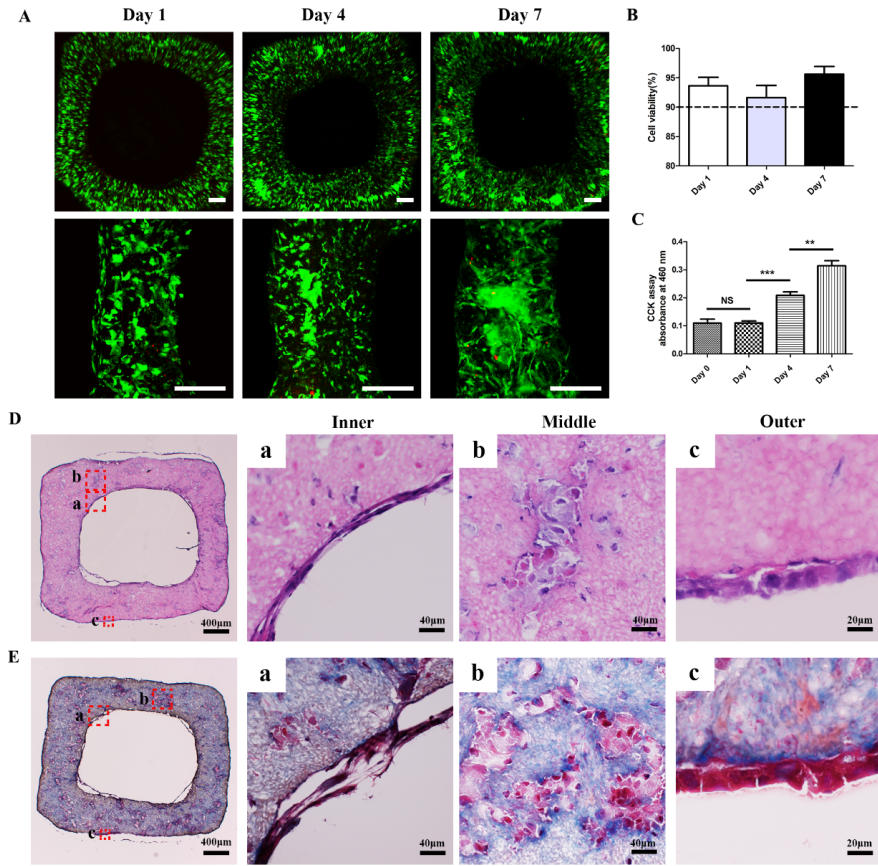


Figure 6

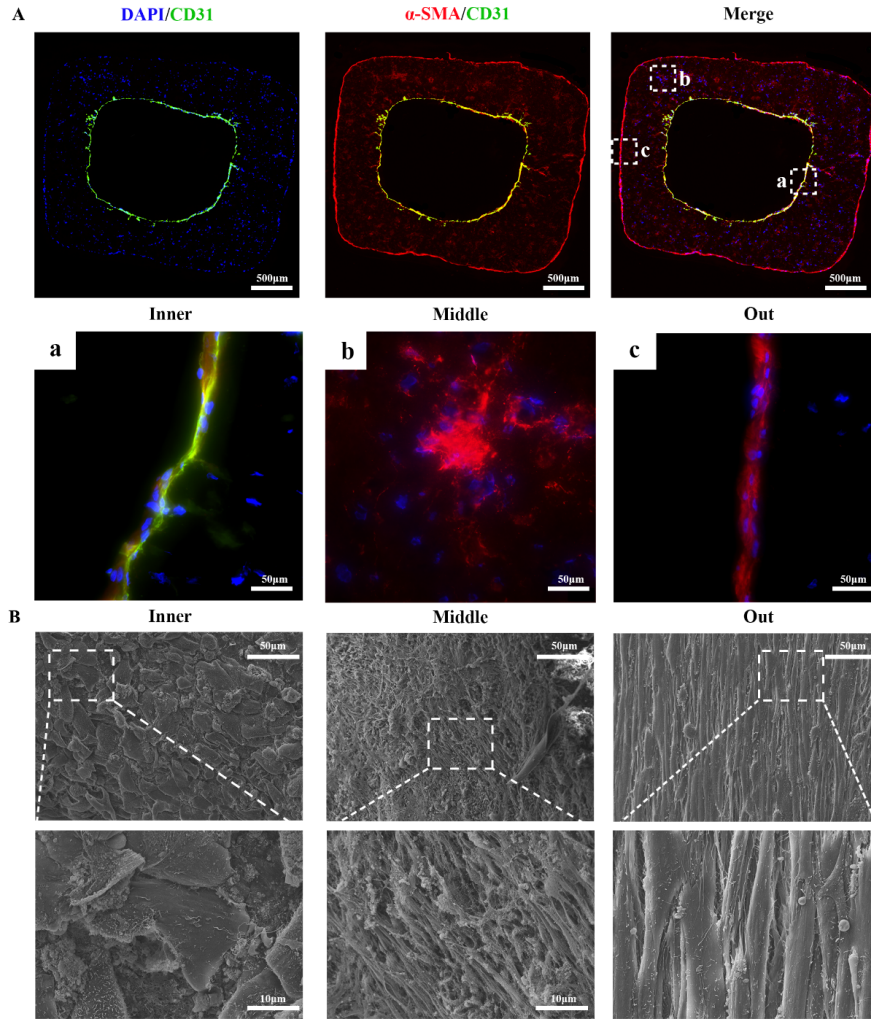


Figure support 1

